



Co-published by
Institute of Fluid-Flow Machinery
Polish Academy of Sciences
Committee on Thermodynamics and Combustion
Polish Academy of Sciences

Copyright©2024 by the Authors under license CC BY 4.0

<http://www.imp.gda.pl/archives-of-thermodynamics/>



Experimental investigation of heat transfer and aerodynamic drag of novel heat sinks with lamellar fins

Aleksandr Terekh, Aleksandr Rudenko, Yevhenii Alekseik*

National Technical University of Ukraine "Igor Sikorsky Kyiv Polytechnic Institute", Educational and Scientific Institute of Atomic and Thermal Energy, 37, Beresteisky Av., Kyiv, 03056, Ukraine

*Corresponding author email: alexeik_kpi@ukr.net

Received: 14.05.2023; revised: 04.07.2023; accepted: 05.10.2023

Abstract

Heat transfer and aerodynamic drag of novel small-sized heat sinks with lamellar fins, designed for electronic cooling, were experimentally investigated under conditions of forced convection in the range of Reynolds numbers 1 250–10 500. It was found that a gradual reduction in the fin spacing from 6 mm to 3 mm with a 29° angle of taper between the outermost fins leads to an increase in the heat transfer intensity by 15–32% with a significant increase in aerodynamic drag compared to the surface with a constant fin spacing of 6 mm. Incomplete cross-section cutting of fins at the relative depth of 0.6 in addition to the gradual reduction in the fin spacing provides aerodynamic drag decrease by 5–20% and increase of heat transfer intensity by 18–20% in comparison with the similar heat sink without fins cutting. Proposed novel designs of heat sinks enabled us to decrease by 7°C–16°C the maximum overheating of the heat sink's base in the flow speed range from 2.5 m/s to 7.5 m/s at constant heat load. To ensure a constant value of maximum overheating of the heat sink base the inlet flow velocity for the surface with constant fin spacing should be 1.6–2 times higher than that for the heat sink with 29° taper angle between outermost fins and partially fins cutting. In this case, the aerodynamic drag for the latter will be higher only by 1.6–2.7 times, which is quite acceptable.

Keywords: Heat sink; Lamellar finning; Electronic cooling; Aerodynamic drag; Heat transfer

Vol. 45(2024), No. 1, 53–63; doi: 10.24425/ather.2024.150438

Cite this manuscript as: Terekh, A., Rudenko, A., & Alekseik, Y. (2024). Experimental investigation of heat transfer and aerodynamic drag of novel heat sinks with lamellar fins. *Archives of Thermodynamics*, 45 (1), 53–63.

1. Introduction

Heat sinks are widely used for cooling various electronic, components (such as power semiconductors, LED, microprocessors, microchips and others) operating with a high specific heat load. To ensure their reliable operation over a long period of time of functioning these devices should be cooled because the failure rate of these components doubles with each increase in temperature by 10°C above the operating temperature (~ 80°C) of the electronic device [1].

Therefore, an important factor during the development of electronic devices is the choice of systems and methods of cooling, providing the most intensive heat removal from heat-loaded components while reducing their mass-size characteristics and minimizing manufacturing costs. In this regard, the development of new designs of heat sinks, allowing the removal of heat by air cooling, becomes relevant in terms of improving the efficiency and durability of electronic devices.

In the paper [2], heat transfer intensity and pressure losses of heat sinks with lamellar, cross-split and pinned fins were investi-

Nomenclature

b	– width of the split fin, m
d	– diameter, m
E	– fin efficiency
Eu	– Euler number
F	– area, cross-section area, m ²
G	– coolant flow rate, kg/s
h	– height, fin height, m
k_u	– conversion factor
L	– length, m
Nu	– Nusselt number
Q	– heat flow, W
Re	– Reynolds number
T	– temperature, K
\bar{T}	– average temperature, K
t	– fin spacing, m
u_c	– cutting width, m
W	– velocity, m/s
w	– base width, m
Z	– number of fins
ΔP	– aerodynamic drag, Pa
ΔT	– overheating, °C

Greek symbols

α	– heat transfer coefficient, W/(m ² K)
β	– angle between fin and wall, °
δ	– thickness, m
λ	– heat conductivity coefficient, W/(m K)
ν	– coefficient of kinematic viscosity, m ² /s
ρ	– density, kg/m ³
φ	– taper angle, °
Ψ	– finning coefficient

Subscripts and Superscripts

1	– inlet of the heat sink
2	– outlet of the heat sink
all	– total
b	– base
c	– cut
f	– fin
h	– hydraulic
los	– losses
max	– maximum
noz	– nozzle
o, on	– inlet of the working section
red	– reduced

gated. The data presented in the paper show that in the range of Reynolds numbers 2 500–14 000, the heat sink with pin and split fins has the lowest thermal resistance. The smallest aerodynamic drag was observed for the lamellar heat sink.

The influence of geometrical characteristics of lamellar-finned heat sinks on heat exchange and pressure drop under conditions of forced convection ($Re = 25\,000$ – $1\,750\,000$) was studied experimentally in [3]. The authors found that the pressure drop along the heat sink increases with increasing fin height, Reynolds number and decreasing inter-fin gap. The average value of Nusselt numbers increases with the increasing Reynolds number, inter-fin gap, fin thickness and with the decreasing fin height.

In [4], on the basis of the lamellar-finned heat sinks, the original design of the combined lamellar-pinned heat sink, the pins of which are located in the gap between the adjacent lamellar fins, is developed. Both numerical and experimental studies of heat transfer and aerodynamic drag of such heat sinks under the conditions of forced convection in the range of flow velocities in the inter-fin gap from 6.5 m/s to 12.5 m/s have been conducted. The results indicate that the thermal resistance of the lamellar-pinned heat sink is about 30% lower than that of the plate-fin heat sink used as the basic one under the conditions of equal velocity of the incoming air flow. It is noted that the pins turbulate the flow in the inter-fin gap. As a result, the intensity of heat exchange increases, but at the same time its aerodynamic drag increases by 2.5–4 times.

Paper [5] presents the results of experimental studies of heat transfer and thermal resistance of plate-fin and lamellar-pinned heat sinks, which are made under conditions of natural convection. The data obtained indicate a higher intensity of heat transfer and lower thermal resistance by 20–40% in the lamellar-pinned heat sink compared with the traditional plate heat sink.

The results of the paper are qualitatively consistent with the results of [4].

The purpose of the study published in [6] is to determine by computational fluid dynamics (CFD) modelling the optimal value of the ratio of the height of the Y-shaped pin fin to the height of the entire fin, which will, according to the authors, increase the cooling efficiency of the pin heat sinks of the new type. Obtained results show that for values of air velocity 0.5–2.5 m/s and the relative height of the pinned Y-fin (height of the straight part of the fin / overall fin height) $H/A = 0.2$ – 0.8 , the optimum ratio of the relative height of fins is $H/A = 0.6$, corresponding to the lowest thermal resistance of a flat heat sink with pinned fins. In our opinion, it would be advisable to compare the received values of thermal resistances with values of resistances of the heat sink at $H/A = 1.0$ which would allow finding out a value of the received effect from the use of the Y-shaped fins.

In [7], the heat transfer and aerodynamic drag of the four designs of new flat lamellar-finned heat sinks with trapezoidal and stepped configurations of lamellar fins in the inlet flow rate variation range from 1 m/s to 5.5 m/s were experimentally studied. It was found that the stepped and trapezoidal fins provide higher thermal conductivity and lower aerodynamic drag compared to the basic plate-fin heat sink at the same flow velocity. The effective conductivity of the trapezoidal fin exceeds the conductivity of the rectangular fin by about 38% at the inlet flow velocity of 5 m/s in spite of the fin area reduction by 20%, and aerodynamic drag is reduced by 20% compared to the conventional plate-fin heat sink.

Studies of the thermo-aerodynamic characteristics and thermal resistance of heat sinks with stepped, trapezoidal plate and plate-fin stepped and trapezoidal fins were conducted in [8] using the CFD method. The results of research testify to the fact that stepped and cut fins allow for increasing the heat transfer

coefficient by 11–16% and decreasing the aerodynamic drag by 15–45% at the reduced area of fins, but at the same time the thermal resistance of heat sinks is increased by 15–25%. Installation of pins in three transverse planes of inter-fin gaps leads to an increase in the intensity of heat transfer by an average of 40% and an increase in aerodynamic drag by 3.5–7 times compared with the traditional lamellar fins, while reducing the thermal resistance by an average of 30–40%.

The paper [9] is aimed at the experimental and numerical study of convective heat transfer and flow characteristics of plate and cross-split finned heat sinks. The cutting width of the fins and the number of the cut fin parts were varied. Investigations were performed at the flow velocity from 1 m/s to 4 m/s and thermal power equal to 100 W. The results showed that the thermal resistance of the heat sink with a 1.5 mm fin width and six cut fin parts is 16.2% lower than that of the heat sink with plate solid fins at the same flow velocity.

In the publication [10], the heat transfer and aerodynamics of a flat tube with both continuous lamellar fins and cut lamellar fins, which were placed on the lateral flat surfaces of the flat tube in in-line and staggered order, were studied using numerical simulation. The authors have shown that full cross-section cutting of fins with a large number of cuts and small width of the cut leads to the intensification of heat exchange and its greatest effect is observed at the staggered arrangement of fins.

In [11], on the basis of collected data from more than 90 publications, the authors reviewed the issues that are aimed at improving the thermal performance of developed heat sinks with pin and lamellar fins by applying various heat exchange intensifiers: perforation in the pins of circular, triangular, rectangular, oval cross-section, turning the pins (not circular cross-section) around their axis by some angle, application of holes to the fins for natural and forced convection conditions.

A lot of publications are dedicated to the investigation of characteristics of small-sized heat dissipating flat surfaces with plate-split fins with the turning of incised parts of fins in relation to flow designed for cooling of electronic devices under forced convection ($Re = 2\ 000\text{--}10\ 000$). Results of the experimental study of heat transfer of such surfaces are presented in [12] and of aerodynamic drag – in [13]. In [14], eight types of surfaces with different cutting depths and angles of turning were experimentally investigated. The influence of fins cutting and turning of cut parts on thermal and aerodynamic characteristics of heat sinks is studied in [15] by means of CFD modelling. The authors [16] have experimentally established that the greatest intensifying effect is observed at a relative depth of fin cutting of 0.6. Partial cutting leads to a 15–20% increase in heat transfer intensity and resistance, and turning of incised parts of fins in relation to flow by angles φ equal to 30° and 45° allows for increasing the heat transfer intensity by 50–60% at a growth of aerodynamic drag by 1.7–2.5 times in comparison with traditional lamellar-finned surfaces. Similar results were obtained in [17] but with the use of CFD modelling. Generalization of experimental data on thermal and aerodynamic characteristics of heat sinks with different types of finning, including fins with partial cut, is presented in [18]. Partially cut fins have also proven themselves

well in studies of thermo-aerodynamic characteristics of transversal finned tube packages. For example, the thermal efficiency of such packages with rolled petal finning was experimentally investigated in [19]. Results of the experimental study of heat transfer of tube packages with split spiral fins were presented in [20] and for aerodynamic drag – in [21]. Summarizing these works it can be said that cutting of fins leads to increasing the heat transfer intensity of tube packages by 30–35% with a moderate increase of aerodynamic drag by 40–45%.

Heat sinks with mesh-wire fins are of certain interest due to their original design. In work [22], materials on experimental research of convective heat transfer and aerodynamic drag of flat heat dissipating surfaces with mesh-wire fins in which geometrical characteristics of mesh fins and flow regime parameters were varied, are presented. Correlations for calculating the heat transfer coefficient for such surfaces based on experimental data are presented in [23]. Mesh-wire fins allow both transverse and longitudinal washing of mesh fins. The advantage of mesh fins is their high specific mass index, but the disadvantages are a rather low efficiency coefficient of mesh fins E , as well as the predisposition to contamination of mesh fins by indoor dust. Therefore, the use of such surfaces is recommended in clean rooms.

Thus, the plate and pin remain the most versatile and widely used fin shape with proven performance, cost and manufacturing techniques. On the other hand, searching for new geometry and shape of fins of the heat sink with the aim of extracting the maximum increase in heat dissipation of the heat sink while reducing (if possible) its aerodynamic drag and improving mass-size indicators is still going on. To meet such requirements, a novel design of heat dissipating surface with lamellar fins and a maximum angle of taper of edge fins 29° was developed [24], and results of its heat transfer characteristics and aerodynamic drag investigation are proposed.

2. Materials and methods

2.1. Research methodology

Studies of convective heat transfer and aerodynamic drag of surfaces with a flat base and lamellar fins under conditions of forced convection were carried out on the experimental setup, which is an open-type wind tunnel of a rectangular cross-section with dimensions (height \times width) 40×85 mm (Fig. 1).

The flow part of the experimental setup consisted of a working section (1) 400 mm long and two calming sections (2) 700 mm long each. The detailed design of the working section is depicted in Fig. 1. The calming sections were intended for the alignment of flow velocity fields and static pressure. The flowing part was connected to the inlet nozzle (5) through the transition diffuser (3). The inlet nozzle was profiled along the lemniscate with an internal diameter of 42 mm. From the other side, the flowing part was connected to the suction centrifugal electric fan (6) through the transition confuser (4). The air flow rate through the fan was regulated smoothly by an autotransformer and by manual-operated dampers (8) to ensure flow rates less than 2 m/s ($W_o < 2$ m/s).

The investigated heat sink (10) was installed in the working section. Heating of the heat sink was carried out with a spiral

ohmic electric heater (12). It was placed inside an insulated casing with an outer diameter of 50 mm. The casing was poured with aluminium oxide powder (Al_2O_3) (13) to ensure uniform heat input and reliable contact between the heater and the base of the heat sink. The casing with the heater was tightly fixed to the centre of the back part of the base (11). An autotransformer

was used to power the heater. The autotransformer was connected to the AC mains through a voltage stabilizer.

To study the aerodynamic drag of heat sinks, two nozzles with a diameter of 1 mm were placed in the walls of the working section at a distance of 50 and 120 mm from the flow inlet and

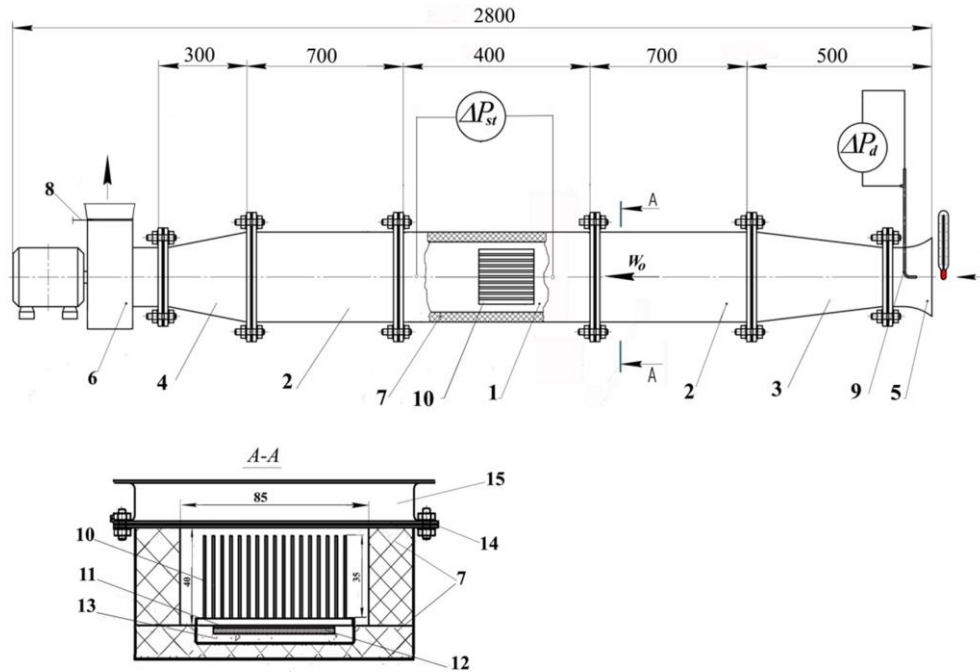


Fig. 1. Experimental setup: 1 – working section; 2 – calming sections; 3 – transition diffuser; 4 – transition confuser; 5 – inlet nozzle; 6 – electric fan; 7 – thermal insulation; 8 – damper; 9 – Prandtl-Pitot tube; 10 – investigated heat sink; 11 – base of the investigated heat sink; 12 – electric heater; 13 – aluminium oxide powder (Al_2O_3); 14 – cover of the working section; 15 – clamping frame.

outlet from the heat sink respectively for taking static pressures. According to the value of pressure difference between the inlet and outlet flow static pressure drops were determined with the help of a micromanometer MMN-240.

Figure 2 shows a photo of the experimental setup consisting of the following measuring instruments:



Fig. 2. Photo of the experimental setup.

- Prandtl-Pitot-Tube and micromanometer MMN-240 with accuracy class 1.0, which were used to determine the dynamic nozzle pressure;
- barometer-aneroid with accuracy class 1.0 to determine the ambient barometric pressure;

- mercury thermometer with a scale value of $0.1^\circ C$ for determining the air temperature at the nozzle inlet;
- a wattmeter with an accuracy class of 0.5 for measuring the electric power supplied to the heater of the surfaces under study;
- multichannel data acquisition module ICP CON I-7018.

Heat sinks of three designs were investigated (Figs. 3 and 4). It should be noted that the only difference between heat sinks of type 2 and type 3 was the fins cutting of the heat sink type 3. The main geometrical characteristics of the heat sinks under study are shown in Table 1.

The lamellar fins were soldered into longitudinal grooves 1 mm deep pre-milled in the base with a fin spacing of $t_1 = 6$ mm for the surface of type 1. For surfaces of types 2 and 3, the fin spacing at the flow inlet into the surface was 6 mm, and starting from the middle fin it decreased gradually on both sides and was 3 mm ($t_2 = 3$ mm) at the outlet of the finned surface. The taper angle between the fins varied from an angle $\varphi = 0^\circ$ (the central fin) to an angle $\beta = 14.5^\circ$ at the outermost fin. The greatest angle of taper between the two outermost fins was 29° ($\varphi = 29^\circ$).

The full areas of the surfaces of types 1 and 2 had close values (the difference is less than 0.8%), in spite of the fact that the base area of the surface of type 2 decreased by $\approx 25\%$. Due to

the gradual increase in the fin length, the difference between the full areas of the surfaces turned out to be insignificant (Table 1).

The total area of the surface of type 3 due to the cutting of fins was decreased relative to that of type 1 by 4.25%.

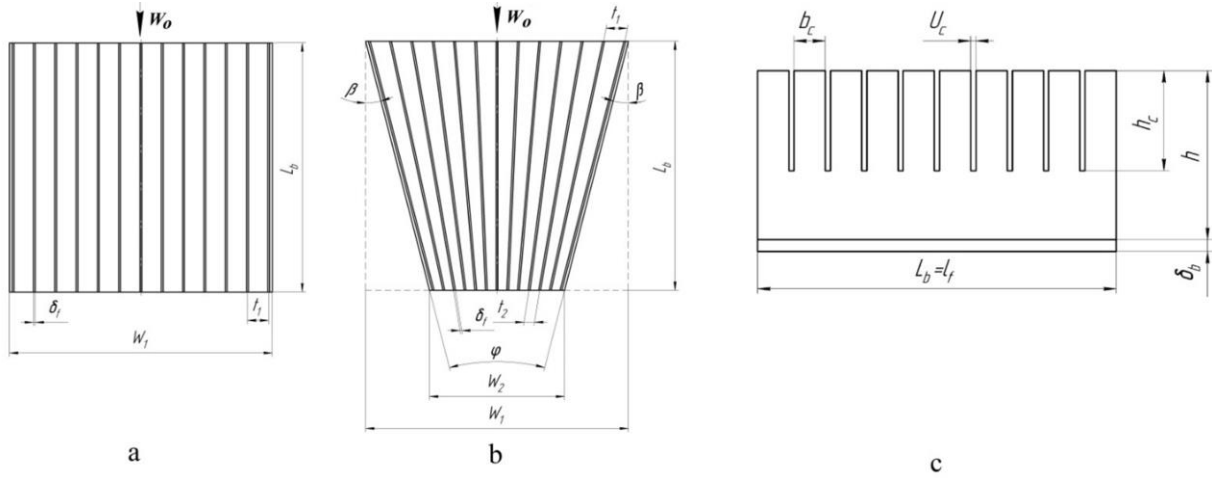


Fig. 3. Design of heat sinks: a – type 1; b – type 2; c – middle fin side view of the heat sink type 3.

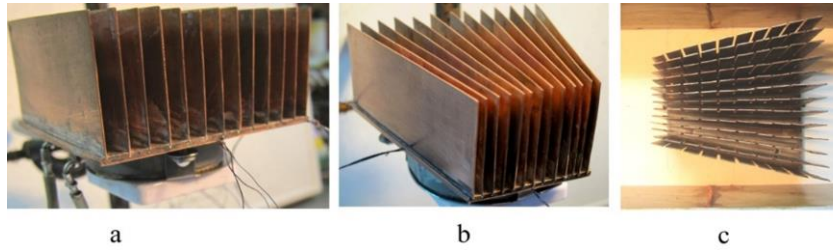


Fig. 4. External view of heat sinks: a – type 1; b – type 2; c – type 3.

Table 1. Geometric characteristics of heat sinks.

#	Parameter	Nomenclature	Units	Experimental heat sink type		
				1	2	3
1	Fin height	h	mm	35.5	35.5	35.5
2	Input/output fin pitch	t_1/t_2	mm	6/6	6/3	6/3
3	Fin thickness	δ_f	mm	0.5	0.5	0.5
4	Middle fin length	l_f	mm	70	70	70
5	Depth of cutting	h_c	mm	-	-	21
6	Cutting width	u_c	mm	-	-	1.0
7	Width of cut fin segments	b_c	mm	-	-	6.1
8	Input/output base width	w_1/w_2	mm	74/74	74/38	74/38
9	Base length	L_b	mm	70	70	70
10	Base thickness	δ_b	mm	2.5	2.5	2.5
11	Number of fins	Z		13	13	13
12	Hydraulic diameter	d_h	mm	11.0	11.0	11.0
13	Total surface area	F_{all}	cm ²	709.7	704.2	679.7
14	Area difference	Δ_F	%		0.8	4.25
15	Finning coefficient	ψ	-	12.03	15.44	14.90
16	Maximal taper angle	φ	degree	0	29	29
17	Surface material	-	-	copper	copper	copper

The finning coefficient (a ratio between the overall area of the finned surface and the area of the surface without finning (base) $\Psi = F_{all}/F_b$) of the type 2 and 3 samples is significantly higher than that of the type 1 sample because of a smaller base area of the type 2 and 3 samples. This parameter is widely used for convective heat transfer calculation of finned tubes [25], data

generalization [26] and investigation of convective heat transfer and aerodynamic drag of bundles of transversely finned tubes [27].

The temperature field of the base of the heat sink surfaces was determined using six (No. 1–6) T-type thermocouples (of wire diameter 0.1 mm), which were placed on the base of the

heat sink as shown in Fig. 5. Additional thermocouples No. 7–8 together with thermocouples No. 1–3 were intended for detecting the temperature changing along the symmetry line and the

air flow direction connected with air velocity change. Signals from thermocouples through a multichannel data acquisition module ICP CON I-7018 were transferred to the computer, automatically recorded and displayed on the computer monitor.

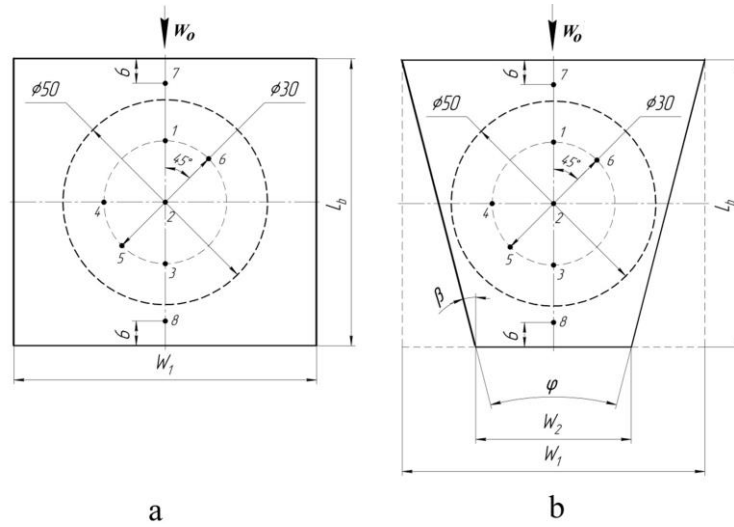


Fig. 5. Location of thermocouples on the heat sink base: a – heat sink type 1; b – heat sink type 2, 3; 1–8 – numbers of thermocouples.

The described above research methodology has such advantages: simplicity, reliability of methodology itself and obtained results. The impossibility of correct defining of contact thermal resistance on the border between the basic surface and fin can be named as a disadvantage of the methodology. This methodology can be applied for experimental investigation of heat and aerodynamic characteristics of flat heat sinks with different types of fins, including applying different heat transfer intensifiers, and heat sinks based on heat pipes.

2.2. Methods of measuring and processing experimental data

The study of patterns of convective heat transfer of heat dissipating surfaces was reduced to determining the dependences of Nusselt numbers, calculated from the reduced convective heat transfer coefficients (α_{red}), on Reynolds numbers.

The average temperature at the base of the heat dissipating surface was calculated as the average of thermocouples 1–6 (Fig. 5), using the ratio:

$$\bar{T}_b = \frac{\sum_{i=1}^N T_i}{N}, \quad (1)$$

where T_i – the base temperature at the mounting points of the thermocouples (1–6), $N = 6$ – the number of thermocouples.

The reduced heat transfer coefficient was determined directly from the results of measuring the temperature field of the heat sink base using the formula:

$$\alpha_{red} = \frac{Q - Q_{los}}{F_{all}(\bar{T}_b - T_{on})}, \quad (2)$$

where Q – power of the electric heater, W ; Q_{los} – heat losses, W ; F_{all} – total area of the heat transfer surface, m^2 ; T_{on} – air temperature at the inlet of the working section, K .

The amount of heat dissipated by the heat sink was determined by the values of electric power supplied to the heater, taking into account the heat loss through the base by heat conduction into the lower wall of the working section of the wind tunnel and the heat that is withdrawn by radiation. Preliminary experiments showed that the value of heat losses of heat sink amounts to 2–3% of the supplied electric power, and the heat dissipated from the surface by radiation did not exceed 2–2.5% of the total heat power dissipated by the heat sink.

The air flow rate in the inlet nozzle was determined by the ratio:

$$W_{noz} = \xi \sqrt{\frac{2g\Delta P_d}{\rho_{noz}}}, \quad (3)$$

where g – gravitational acceleration, m/s^2 ; ΔP_d – difference of full and static pressure, Pa , ρ_{noz} – air density in the nozzle, kg/m^3 , $\xi = 0.99$ – correction factor, set on the basis of calibration of the Pitot-Prandtl tube.

According to the continuity equation, the flow velocity at the inlet to the working section before the heat sink was determined by the equation:

$$W_o = k_u \cdot W_{noz}, \quad (4)$$

where k_u – is the coefficient, which is defined as:

$$k_u = F_{noz}/F_{on}, \quad (5)$$

where F_{noz} – nozzle cross-section area, m^2 ; F_{on} – cross-section area at the inlet of the working section, m^2 .

The air flow rate G in the cross-section of the working section was determined by the following dependence:

$$G = \rho_{noz} W_{noz} F_{noz}. \quad (6)$$

The hydraulic diameter of the heat sink cross-section d_h at the inlet ($d_h = 11$ mm) was taken as a defining size in Nusselt and Reynolds numbers, which proved to be good for defining size in similarity numbers [28]. The velocity in the working channel in front of the heat sink surface W_o was taken as a characteristic air velocity. The physical properties of air λ , ν , which are included in the expressions for the numbers Nu and Re , were related to the flow temperature at the inlet to the heat sink surface. The Nusselt and Reynolds numbers were determined as:

$$Nu_{red} = \frac{\alpha_{red} \cdot d_h}{\lambda}, \quad (7)$$

$$Re_e = \frac{W_o \cdot d_h}{\nu}, \quad (8)$$

where λ – air heat conductivity, $W/(m \cdot K)$; ν – air kinematic viscosity, m^2/s .

The aerodynamic drag of the investigated heat sinks was determined in the conditions of isothermal flow at air temperatures $T_o = 290$ – 300 K. Pressure losses caused by the heat sink were defined with taking into account friction pressure losses in the working section:

$$\Delta P = \Delta P_{stat} - \Delta P_{fric}, \quad (9)$$

where ΔP_{stat} – static pressure difference, Pa; ΔP_{fric} – friction pressure losses, Pa.

Based on ΔP values, the values of Euler's number Eu were determined:

$$Eu = \frac{\Delta P}{\rho_{noz} W_o^2}. \quad (10)$$

2.3. Uncertainty analysis

In this work, uncertainty analysis of direct and indirect measurements was performed according to main recommendations of [29]. Direct measurements in this study include measurements of geometric parameters of the experimental setup and heat sinks, static and dynamic pressures, temperatures and heater electric power. Indirectly measured values are determined by calculations based on the results of direct measurements. These include: heat transfer coefficients α , flow velocity W , numbers: Reynolds Re , Nusselt Nu , Euler Eu .

The general uncertainty of a direct measurement consists of systematic and random errors [30]. Primary analysis of the experimental data has shown that the order of systematic and random errors is the same as for surface temperature measurement. Uncertainty of the other measurements was defined mainly by systematic errors connected with measurement apparatus errors and imperfection of the measurement method. The error of heat sinks geometrical parameters measurement was ± 0.05 mm. Errors of direct measurements of regime parameters were defined by the accuracy class of measurement apparatus and chosen range of measurement.

The error of determining the surface temperature consists of the absolute error of thermocouples measurement and the error of thermocouples calibration. The absolute error of thermocouples measurement was equal to 0.25 K. The error of thermocou-

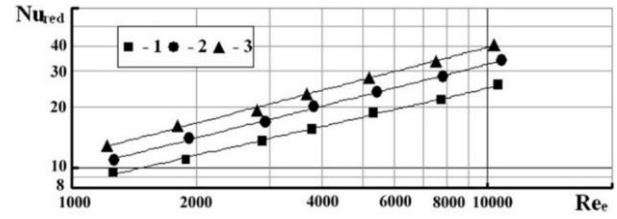


Fig. 6. Results of the study of heat sinks heat transfer: 1 – heat sink type 1; 2 – heat sink type 2; 3 – heat sink type 3.

ple calibration is not more than 0.2 K when an exemplary platinum-platinum-rhodium thermocouple is used for calibration. Then the absolute error of measurement of surface temperatures was:

$$e = [(0.25)^2 + (0.2)^2]^{0.5} \approx 0.3 \text{ K}. \quad (11)$$

The uncertainty of overall heat quantity which was transferred to the air was $\pm 2.5\%$.

Experimental data of heat transfer investigation were used to calculate the uncertainty of the reduced heat transfer coefficient α_{red} and the corresponding Nusselt number.

The uncertainty of determining the Euler number is mainly related to the error in measuring the static pressure differences ΔP_{stat} before and after the lamellar-finned surface.

The stability and repeatability of obtained data was ensured by multiple measurements of parameters. Thus, the duration of temperature measurement at a steady state condition was 1.5–2 minutes which corresponded to 90–120 measurements, and fluctuations of inlet air temperature were insignificant (± 0.3 K).

Performed calculations have shown that the relative uncertainty of the definition of heat transfer coefficient was not more than $\pm(5.4$ – $6.7)\%$, of the Nusselt number $\pm(6.5$ – $7.5)\%$, uncertainty of Reynolds number calculation was not more than $\pm 5.5\%$ and for Euler number $\pm(10$ – $15)\%$.

3. Results and discussion

3.1. Heat transfer

The research of heat transfer was performed in the range of Reynolds numbers $Re_e = 1250$ – 10500 . It was intended to obtain the dependencies between the Nusselt numbers and Reynolds numbers of such a type:

$$Nu_{red} = C_q \cdot Re_e^m, \quad (12)$$

where C_q – coefficient.

Experimental results for heat sinks of types 1–3 are shown in Fig. 6. Analysis of the data presented in Fig. 6 indicates that a gradual decrease in the fin spacing from 6 mm to 3 mm of heat sink type 2 leads to an increase in the intensity of heat transfer by 15–32% compared to the heat sink type 1 with constant fin

spacing (6 mm) due to a gradual increase in velocity in the inter-fin channels. The flow velocity increased 2 times from the inlet to the outlet ($t_1 = 6$ mm, $t_2 = 3$ mm).

Increasing the heat transfer intensity due to fin cutting (heat sink type 3) is explained as follows. The thickness of the boundary layer on the fins increases as flow moves along them when flowing on the type 1 heat sink (without fins cutting). This leads to the deterioration of heat transfer between fins and air flow. Partial cutting of fins into narrow sections, as it was done on the type 3 sample, leads to: destruction of the growing boundary layer, its disruption from the edges of the cut narrow parts, splitting it into thinner sections, increasing the flow disturbance in the area of fins cutting [15]. The combination of these factors and increasing the flow velocity in the inter-fin channels leads to an increase of the heat transfer intensity of the heat sink of type 3 by 35–55% in comparison with that of type 1.

Values of the exponent m in Eq. (12) for all investigated heat sinks exhibit small differences, but the tendency of their increasing is observed (Table 2).

3.2. Aerodynamic drag

Figure 7 presents the results of studies of aerodynamic drag of heat sinks of types 1–3 in the form of dependencies of Euler numbers (Eu) on Reynolds numbers (Re_e). These results can be generalized with such a function:

$$Eu = C_S \cdot Re_e^{-n}, \quad (13)$$

where C_S – coefficient. Table 2 shows values of the exponent n and the C_S coefficient in Eq. (13).

Table 2. Values of the exponents m , n and coefficients C_q , C_S in Eqs. (12) and (13).

Heat sink type	t_1/t_2 m/mm	h_c/h	m	C_q	n	C_S
1	6/6	-	0.4715	0.3210	0.2409	1.7672
2	6/3	-	0.5188	0.2777	0.2268	12.259
3	6/3	0.6	0.5333	0.2894	0.1540	5.9526

The data in Fig. 7 demonstrate a high aerodynamic drag of heat sinks type 2 and 3, which is 7.5 times higher than that of type 1.

A high aerodynamic drag of the type 2 heat sink is connected with a gradually increasing velocity in the narrowing channels between the fins in which the outlet velocity is 2 times higher than the inlet velocity. Some decrease in the aerodynamic drag by 6–15% of the type 3 heat sink is connected, in our opinion, with the air flowing mainly from the inter-fin gaps of the outermost fins into the expanding channel formed by the straight side walls of the channel and the outermost fins, which resulted in a decreasing of the speed in the outermost inter-fin channels of the heat sink.

The proposed forms of correlations for heat transfer (12) and aerodynamic drag (13) are suitable for a wide range of heat sink geometrical sizes and fins quantity. But in some cases, additional experimental investigations are necessary for the specification of coefficients C_q , C_S and exponents m and n . Coefficients

and exponents listed in Table 2 are applicable to heat sinks with the same ratio between the height, length, thickness and fin pitch, the same taper angle and relative depth of fin cutting as for the investigated heat sinks. Taking into account that the hydraulic diameter d_h was chosen as a defining size of Re and Nu numbers, significant changes in heat sink geometry need the correction of coefficients and exponents by means of additional study. It should be noted that the geometrical form of the heater does not influence the form of correlations for heat transfer and aerodynamic drag, but values of the base temperature and their distribution depend on the method of heating and additional investigations are necessary for their defining in any single case.

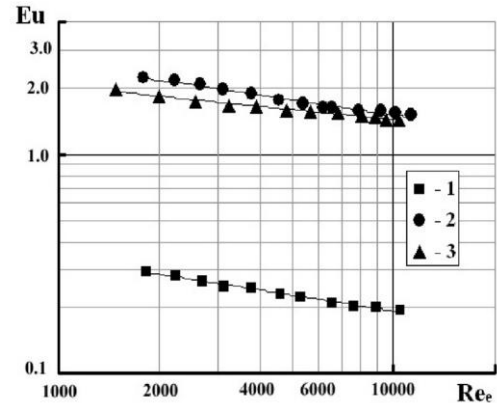


Fig. 7. Results of the study of aerodynamic drag of heat sinks: 1 – heat sink type 1; 2 – heat sink type 2; 3 – heat sink type 3.

3.3. Overheat temperature of heat sink base

One of the main parameters for the evaluation and selection of a finned sink for electronics cooling is the base overheating temperature ΔT at a given heat flow Q , which is removed from the heat loaded electronic components to the base of the heat sink. We distinguish between an average overheating temperature of the base and a maximum overheating temperature. The average overheating temperature is the difference between the average temperature of the base, which is averaged over the readings of thermocouples located on the base, and the value of the cooling medium temperature T_{on} : $\Delta \bar{T}_b = \bar{T}_b - T_{on}$. The maximum overheating temperature of the base is the difference between the maximum temperature of the base and the cooling medium temperature (air temperature at the inlet to the heat sink).

Figure 8 shows changes of the overheating temperature along the flow direction in the inter-fin channels of heat sinks type 1–3 according to the readings of thermocouples T1–T3, T7, T8 (Fig. 5). The dashed vertical lines indicate the boundaries of the heat sink, and lines I–I and II–II are the boundary within which the electric heater is installed on the base.

The curves $\Delta T = f(L)$ for the three types of heat sinks are qualitatively similar. At the inlet of the flow, the base overheating temperature is lower, because the flow has the air inlet temperature (T7), and as it moves deeper, it warms up, and the temperature of the base increases and has a maximum in the centre of the heater at point T2. Further, as the flow moves toward the outlet, the overheating temperature decreases slightly at point

T3, and at the outlet of the inter-fin channels has a temperature 3°C less than at point T2 for the type 1 heat sink. The overheating of the base of the type 1 heat sink remains high due to the fact that the average flow velocity in the inter-fin channels remains approximately constant. The overheating temperatures along the symmetry axis of the type 2 and 3 heat sinks differ significantly from the overheating temperatures of the type 1

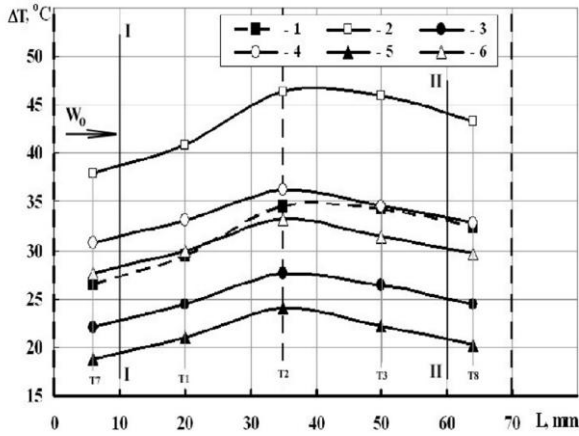


Fig. 8. Dependence of the overheating temperature ΔT of the heat sink base along the longitudinal axis of symmetry on the base length L at $Q = 100$ W: 1, 2 – heat sink of type 1 at W_o values 7.35 and 3.96 m/s; 3, 4 – heat sink of type 2 at W_o values 7.35 and 3.98 m/s; 5, 6 – heat sink of type 3 at W_o values 7.48 and 4.03 m/s; T1–T3, T7, T8 – numbers of thermocouples according to Fig. 5; I-I, II-II – boundaries of the electric heater body.

heat sink due to gradual narrowing of inter-fin channels from $t_1 = 6$ mm to $t_2 = 3$ mm and increase in velocity at the outlet by 2 times. For this reason, the level of overheating temperatures decreases at point T2 by 7°C and 10°C for heat sinks of type 2 and 3, respectively at inlet flow velocity $W_o \approx 7.4$ m/s.

For the air velocity $W_o \approx 4$ m/s, decreasing the overheating temperature in point T2 for heat sinks of type 2 and 3 in comparison with the heat sink of type 1 is 10°C and 13°C, accordingly. The type 3 heat sink with transverse incompletely cut fins has the lowest maximum overheating temperature at point T2 of the heat sinks compared. This can be explained by turbulizing of the flow due to its disruption from the edges of the incised parts of the fins, which leads to an increase in the intensity of heat transfer, while the temperature of the base decreases. In general, the level of temperature overheating along the length of the base for heat sinks of type 2 and 3 is significantly lower than that for the heat sink of type 1 at the same flow velocities and heat flow value of $Q = 100$ W.

Figure 9 shows experimental data for the dependence of the maximum overheating temperature of the base ΔT_{max} on the flow velocity at the inlet to the heat sink W_o .

Maximum overheating temperatures of the base for the three types of heat sinks decrease with the increasing speed, but the level of temperature overheating significantly differs. For heat sinks of type 2 and 3, the values of ΔT_{max} are 7.5–10°C lower and 10–13°C lower, respectively, than those of heat sink type 1. The explanation of this difference is the same as the described above difference between curves $\Delta T = f(L)$ depicted in Fig. 8.

The results presented in Fig. 9 also show that in order to achieve a constant maximum overheating temperature equal to $\Delta T_{max} = 40^\circ\text{C}$ for the type 1 heat sink, the inlet air velocity must

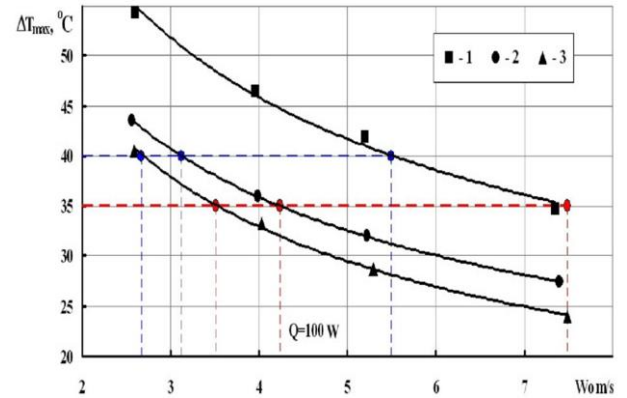


Fig. 9. Dependence of the maximum overheating temperature of the base ΔT_{max} on the flow velocity W_o at the inlet at $Q = 100$ W: 1 – heat sink of type 1; 2 – heat sink of type 2; 3 – heat sink of type 3.

Table 3. Comparison of the obtained data at the same Q and ΔT_{max} .

Heat sink type	Q , W	ΔT_{max} , °C	W_o , m/s	ΔP , Pa	$\Delta P_i / \Delta P_1$
1	100	40.0	5.49	9.1	1.0
2	100	40.0	3.12	25.4	2.79
3	100	40.0	2.67	14.0	1.54
1	100	35.0	7.48	15.5	1.0
2	100	35.0	4.24	42.4	2.74
3	100	35.0	3.51	24.0	1.55

be at least $W_o = 5.5$ m/s, for type 2 – $W_o = 3.12$ m/s, for type 3 – $W_o = 2.67$ m/s. For the maximum overheating temperature of the base $\Delta T_{max} = 35^\circ\text{C}$, the inlet flow velocities should be for the type 1 heat sink equal to $W_o = 7.48$ m/s, for type 2 – $W_o = 4.24$ m/s and for type 3 – $W_o = 3.51$ m/s (Table 3). Conclusively, we can say that the novel heat sinks of types 2 and 3 significantly reduce the maximum overheating temperature of the base.

The dependence of pressure loss ΔP on the inlet flow velocity W_o is depicted in Fig. 10. The dashed lines highlight the values of pressure losses at the maximum overheating temperature $\Delta T_{max} 35^\circ\text{C}$ and 40°C . The relative growth of pressure losses at overheating of the base $\Delta T_{max} 40^\circ\text{C}$ and 35°C is 2.74–2.79 times and 1.5 times for heat sinks of type 2 and 3, respectively (Table 3), which is quite acceptable.

4. Conclusions

Novel heat sinks with lamellar fins and variable fin spacing, designed for electronics cooling, have a high heat transfer intensity.

Gradually reducing the fin spacing leads to an increase in the heat transfer intensity by 15–30%.

The combination of factors of speed increasing in inter-fin gaps and partially cutting of fins allows us to increase the heat transfer intensity by 35–55% in comparison with the heat transfer intensity of traditional heat sinks with lamellar fins.

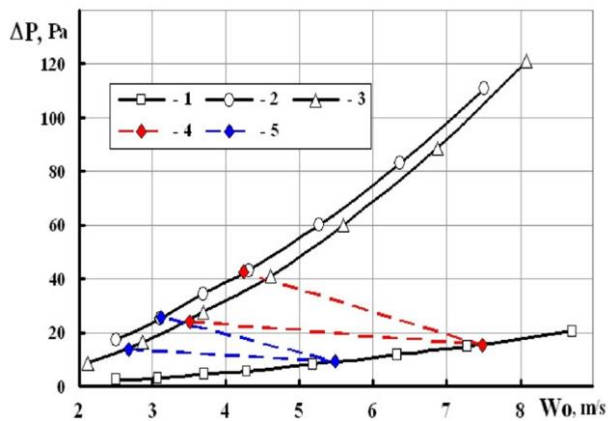


Fig. 10. Dependence of the pressure loss ΔP on the inlet flow velocity W_0 : 1 – heat sink of type 1; 2 – heat sink of type 2; 3 – heat sink of type 3; 4 – $\Delta T_{max} = 35^\circ\text{C}$, $Q = 100\text{ W}$; 5 – $\Delta T_{max} = 40^\circ\text{C}$, $Q = 100\text{ W}$.

The aerodynamic drag of heat sinks with the gradually decreasing spacing between the fins increases by 7–7.5 times relative to the drag of traditional heat dissipating surfaces with lamellar fins.

The maximum overheating temperature of the base for the novel heat dissipating surfaces with gradually decreasing spacing between the fins is 7–13°C lower than that for traditional heat sinks with lamellar fins.

The pressure losses for the novel heat sinks at the same heat load and overheating temperature of the base are significantly reduced from 7–7.5 times to 1.54–2.74 times.

Novel designs of heat sinks allow for improving the mass-size indices by 20–25% at equal conditions.

References

- [1] Gurrum, S.P., Suman, S.K., Joshi, Y.K., & Fedorov, A.G. (2004). Thermal Issues in Next-Generation Integrated Circuits. *IEEE Transactions on Device and Materials Reliability*, 4(4), 709–714. doi: 10.1109/tdmr.2004.840160
- [2] Jonsson, H., & Moshfegh, B. (2001). Modeling of the thermal and hydraulic performance of plate fin, strip fin, and pin fin heat sinks-influence of flow bypass. *IEEE Transactions on Components and Packaging Technologies*, 24(2), 142–149. doi: 10.1109/6144.926376
- [3] El-Sayed, S.A., Mohamed, S.M., Abdel-latif, A.M., & Abouda, A.E. (2002). Investigation of turbulent heat transfer and fluid flow in longitudinal rectangular-fin arrays of different geometries and shrouded fin array. *Experimental Thermal and Fluid Science*, 26(8), 879–900. doi: 10.1016/s0894-1777(02)00159-0
- [4] Yu, X., Feng, J., Feng, Q., & Wang, Q. (2005). Development of a plate-pin fin heat sink and its performance comparisons with a plate fin heat sink. *Applied Thermal Engineering*, 25(2–3), 173–182. doi: 10.1016/j.applthermaleng.2004.06.016
- [5] Haghighi, S.S., Goshayeshi, H.R., & Safaei, M.R. (2018). Natural convection heat transfer enhancement in new designs of plate-fin based heat sinks. *International Journal of Heat and Mass Transfer*, 125, 640–647. doi: 10.1016/j.ijheatmasstransfer.2018.04.122
- [6] Lekaphol, T., Sompong, P., & Srisomporn, S. (2019). Optimal height ratio of Y-shape pin fin to plate fin of PPFHS. *IOP Conference Series: Materials Science and Engineering*, 501, 012062. doi: 10.1088/1757-899x/501/1/012062
- [7] Chen, C.H., & Wang, C.C. (2015). A novel trapezoid fin pattern applicable for air-cooled heat sink. *Heat and Mass Transfer*, 51(11), 1631–1637. doi: 10.1007/s00231-015-1666-4
- [8] Muneeshwaran, M., Sulaiman, M.W., Hsieh, C.H., Chai, M.L., & Wang, C.C. (2022). Heat transfer augmentation of heat sinks through increasing effective temperature difference. *Journal of Enhanced Heat Transfer*, 29(5), 37–55. doi: 10.1615/jenhheat-transf.2022042106
- [9] Chingulpitak, S., Chimres, N., Nilpueng, K., & Wongwiset, S. (2016). Experimental and numerical investigations of heat transfer and flow characteristics of cross-cut heat sinks. *International Journal of Heat and Mass Transfer*, 102, 142–153. doi: 10.1016/j.ijheatmasstransfer.2016.05.098
- [10] Feng, L., Du, X., Yang, Y., & Yang, L. (2011). Study on heat transfer enhancement of discontinuous short wave finned flat tube. *Science China Technological Sciences*, 54(12), 3281–3288. doi: 10.1007/s11431-011-4572-0
- [11] Dhaiban, H.T., Hussein, M.A. (2019). The optimal design of heat sinks: A Review. *Journal of Applied and Computational Mechanics* 6(4), 1030–1043. doi: 10.22055/JACM.2019.14852
- [12] Pismenniy, Ye.N., Burley, V.D., Terekh, A.M., Baranyuk, A.V., Tsvyashchenko, Ye.V. (2005). Heat transfer of flat-plating surfaces with cut fins at force convection. *Promyshlennaya teplotekhnika*, 27(4), 11–16 (in Russian).
- [13] Baranyuk, A.V., Pismenniy, Ye.N., Terekh, A.M., Rohachev, V.A., Burley, V.D. (2006). Aerodynamic drag of flat-plating surfaces with cut fins at force convection. *Promyshlennaya teplotekhnika*, 28(4), 29–33 (in Russian).
- [14] Pis'mennyi, E.N., Rogachev, V.A., Terekh, A.M., Polupan, G., Carvajal-Mariscal, I., & Nezymb, V. (2006). An experimental study of enhancement of forced convection heat transfer from parallel plate fins with cuts. *Annals of the Assembly for International Heat Transfer Conference 13*. Begell House Inc. doi: 10.1615/ihtc13.p17.220
- [15] Baranyuk, A.V., Nikolaenko, Y.E., Rohachov, V.A., Terekh, A. M., & Krukovskiy, P.G. (2019). Investigation of the flow structure and heat transfer intensity of surfaces with split plate finning. *Thermal Science and Engineering Progress*, 11, 28–39. doi: 10.1016/j.tsep.2019.03.018
- [16] Baranyuk, A.V., Rogachev, V.A., Zhukova, Y.V., Terekh, A.M., & Rudenko, A.I. (2020). Experimental investigation of heat transfer of plane heat-removing surfaces with plate finning. *Journal of Engineering Physics and Thermophysics*, 93(4), 962–972. doi: 10.1007/s10891-020-02196-3
- [17] Nikolaenko, Yu., Baranyuk, A., Rohachev, V., & Terekh, A. (2020). Numerical study of heat and aerodynamic drag of the radiator with lamellar split finning. *Archives of thermodynamics*, 41(1), 67–93. doi: 10.24425/ather.2020.132950
- [18] Rohachev, V.A., Terekh, O.M., Baranyuk, A.V., Nikolaenko, Y.E., Zhukova, Y.V., & Rudenko, A.I. (2020). Heataerodynamic efficiency of small size heat transfer surfaces for cooling thermally loaded electronic components. *Thermal Science and Engineering Progress*, 20, 100726. doi: 10.1016/j.tsep.2020.100726
- [19] Pis'mennyi, E.N., Terekh, A.M., & Rogachev, V. A. (1997). New Heat-Transfer Surfaces Made of Tubes with Rolled Petal Finning. *Heat Transfer Research*, 28(4-6), 398–401. doi: 10.1615/heat-transres.v28.i4-6.270
- [20] Terekh, A.M., Shapoval, O.E., & Pis'mennyi, E.N. (2001). The average-superficial heat exchange in banks of in-line tubes with split spiral fins in cross-flow. *Promyshlennaya teplotekhnika*, 23(1-2), 35–41 (in Russian).
- [21] Shapoval, O.E., Pis'mennyi, E.N., & Terekh, A.M. (2001). Aerodynamic drag of transversely streamlined of in-lined tube bundles with split fins. *Promyshlennaya teplotekhnika*, 23(4-5), 63–68 (in Russian).

- [22] Pismennyi, E.N., Rohachev, V.A., Terekh, A.M., Burley, V.D., & Razumovskyi, V.G. (2002). Heat transfer of flat surfaces with mesh-and-wire finning at forced convection. *Promyshlennaya teplotekhnika*, 24(4), 71–78 (in Russian).
- [23] Pis'mennyi, E.N., Terekh, A.M., Rogachev, V.A., Burlei, V.D., & Rudenko, A.I. (2005). Calculation of Convective Heat Transfer of Plane Surfaces with Wire-Net Finning Immersed in a Cross-Flow. *Heat Transfer Research*, 36(1-2), 39–46. doi: 10.1615/heattransres.v36.i12.60
- [24] Nishchik, A.P., Terekh, A.M., Rudenko, A.I., & Vozniuk, M.M.: *Lamellar-finned heat exchange surface*. Ukraine utility model patent. UA 140448 U, Feb. 25, 2020 (in Ukrainian).
- [25] Yudin, V.F. (1982). *Heat Transfer in Cross-Finned Tubes*. Mashinostroenie, Leningrad (in Russian).
- [26] Pis'mennyi, E.N., Terekh, A.M. (1993). Generalized method for convective heat transfer calculation in transversely streamed tube bundles with external ring and spiral-strip fins. *Teploenergetika*, 5, 52-56 (in Russian).
- [27] Pis'mennyi, E. N. (2016). Study and application of heat-transfer surfaces assembled from partially finned flat-oval tubes. *Applied Thermal Engineering*, 106, 1075–1087. doi: 10.1016/j.applthermaleng.2016.06.081
- [28] Pis'mennyi, E. N., Terekh, A. M., Polupan, G. P., Carvajal-Mariscal, I., & Sanchez-Silva, F. (2014). Universal relations for calculation of the drag of transversely finned tube bundles. *International Journal of Heat and Mass Transfer*, 73, 293–302. doi: 10.1016/j.ijheatmasstransfer.2014.02.013
- [29] *ISO Guide to the Expression of Uncertainty in Measurement*. International Organization for Standardization (ISO), Geneva 1993 (Corrected and Reprinted 1995).
- [30] Taylor, J.R. (1997). *Introduction to error analysis, the study of uncertainties in physical measurements*. University Science Book, Sausalito.